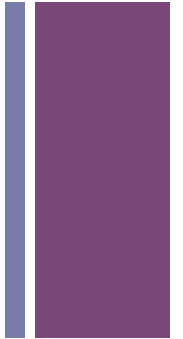


Improving ZZh coupling measurement through ZZ fusion channel at ILC

Based on work with T. Han, Z. Liu and J. Sayre
arXiv: 1504.01399

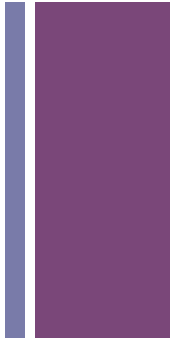
+ Contents:

- Introduction
 - Inclusive cross section
 - ILC
- Analysis
 - Signal, Background
 - Kinematic Variables, Cuts and Distribution
 - Multivariate log-likelihood analysis
- Results
- Possible constraints on dim-6 Operators



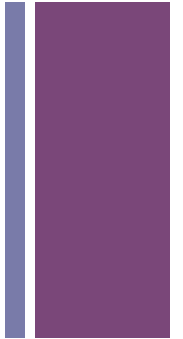


Main Results: Improved sensitivity on Higgs width and couplings:



Relative Error %	ILC 250+500		ILC 250+500+1000	
$\delta\sigma_{Zh}$	6.0%		2.5%	
Improvement		with HL-LHC		with HL-LHC
Γ	4.8 \rightarrow 4.7	4.8 \rightarrow 4.6	4.5 \rightarrow 3.7	4.5 \rightarrow 3.7
g_Z	0.99 \rightarrow 0.94	0.99 \rightarrow 0.94	0.98 \rightarrow 0.75	0.98 \rightarrow 0.75
g_W	1.1 \rightarrow 1.1	1.1 \rightarrow 1.1	1.1 \rightarrow 0.89	1.1 \rightarrow 0.88
g_b	1.5 \rightarrow 1.5	1.5 \rightarrow 1.5	1.3 \rightarrow 1.2	1.3 \rightarrow 1.1

Table 6. The improvement on selected coupling precisions by incorporating our ZZ fusion analysis from a typical 10-parameter model-independent fit. We show both the ILC exclusive results and ILC combined with the optimistic CMS HL-LHC input [27]. For details of fitting scheme and combination scheme, see Ref. [16]. The results for ILC 250/500/1000 (GeV) assume 250/500/1000 fb^{-1} integrated luminosities.



- Higgs Precision measurement

- A light Higgs at 125.09 ± 0.21 (stat.) ± 0.11 (syst.) GeV

(CMS+ATLAS)

- Poorly constrained width accommodates potentially BSM physics.

- From previous analysis (ILC included), the model independent Higgs width is constrained to $\sim 5\%$.



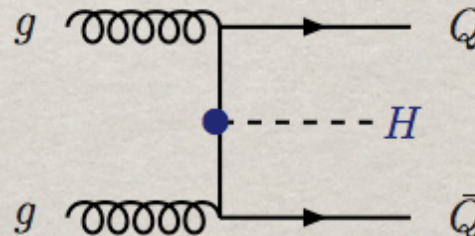
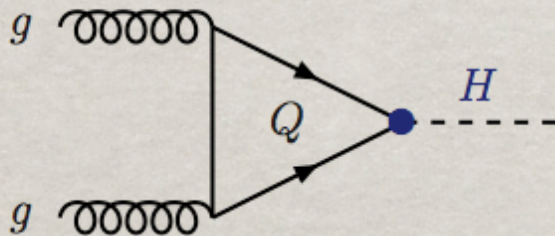
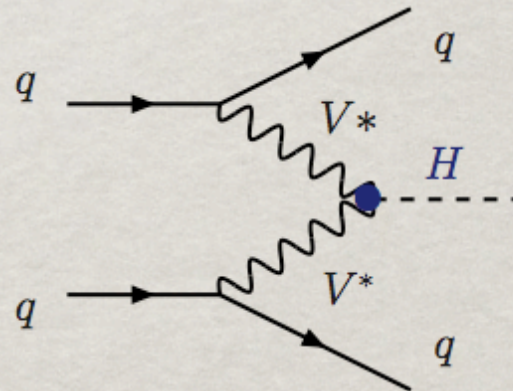
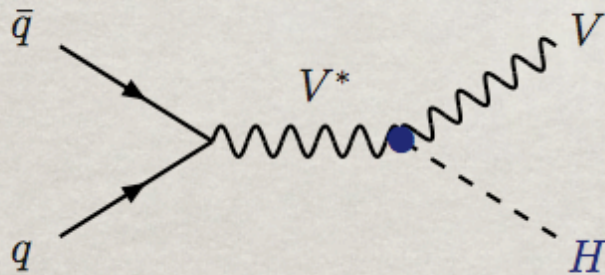
Higgs production at the LHC:

associated production with W/Z : $q\bar{q} \longrightarrow V + H$

vector boson fusion : $qq \longrightarrow V^*V^* \longrightarrow qq + H$

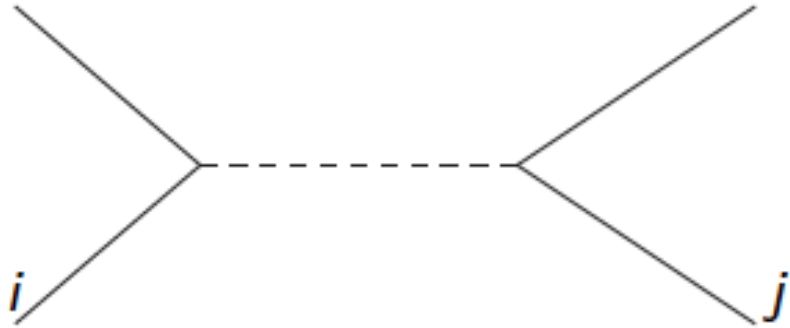
gluon - gluon fusion : $gg \longrightarrow H$

associated production with heavy quarks : $gg, q\bar{q} \longrightarrow Q\bar{Q} + H$



■ Credit: Higgs production at the LHC, T. Han

+ Problems



$$\sigma_{ij} \propto \frac{g_i^2 g_j^2}{\Gamma} \quad (\text{NWA})$$

“Scaling degeneracy”

Solution

Inclusive Higgs
Production Cross section
from the Higgs coupling
to \bar{A} :

$$\sigma_A^{inc} \propto g_A^2$$

- Potential precision on Higgs couplings and total width at the ILC, T. Han, Z. Liu, J. Sayre

+ ILC collider

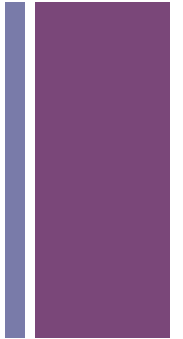
(International Linear Collider)

A linear lepton ($e^+ e^-$) collider

Advantages:

Definite initial state: e^- , e^+

Definite center of mass energy: \sqrt{s}

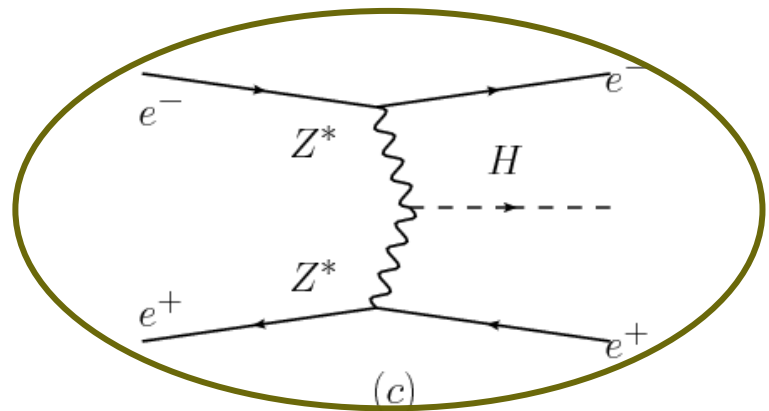
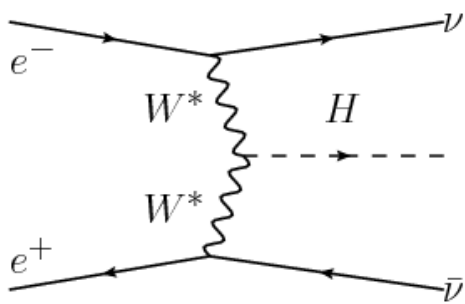
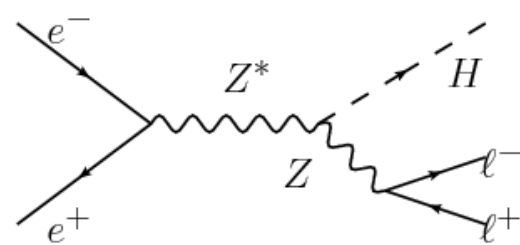
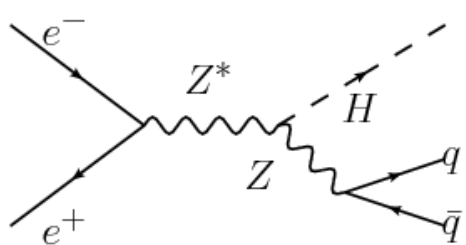
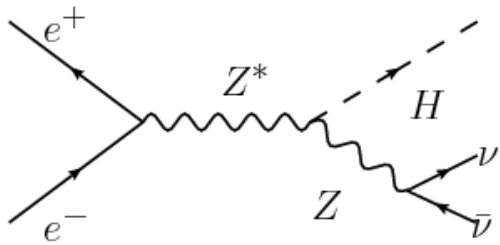
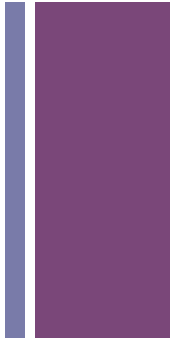


+ Previous study:

- Inclusive cross-section σ_A^{inc} can be measured to relative errors 2.6% and 3%, from studying “Higgsstrahlung” channel at 250Gev and 500Gev ILC.
- Suggested to look at ZZ fusion channel



Higgs Production at an $e^+ e^-$ collider



(a)

(b)

(c)

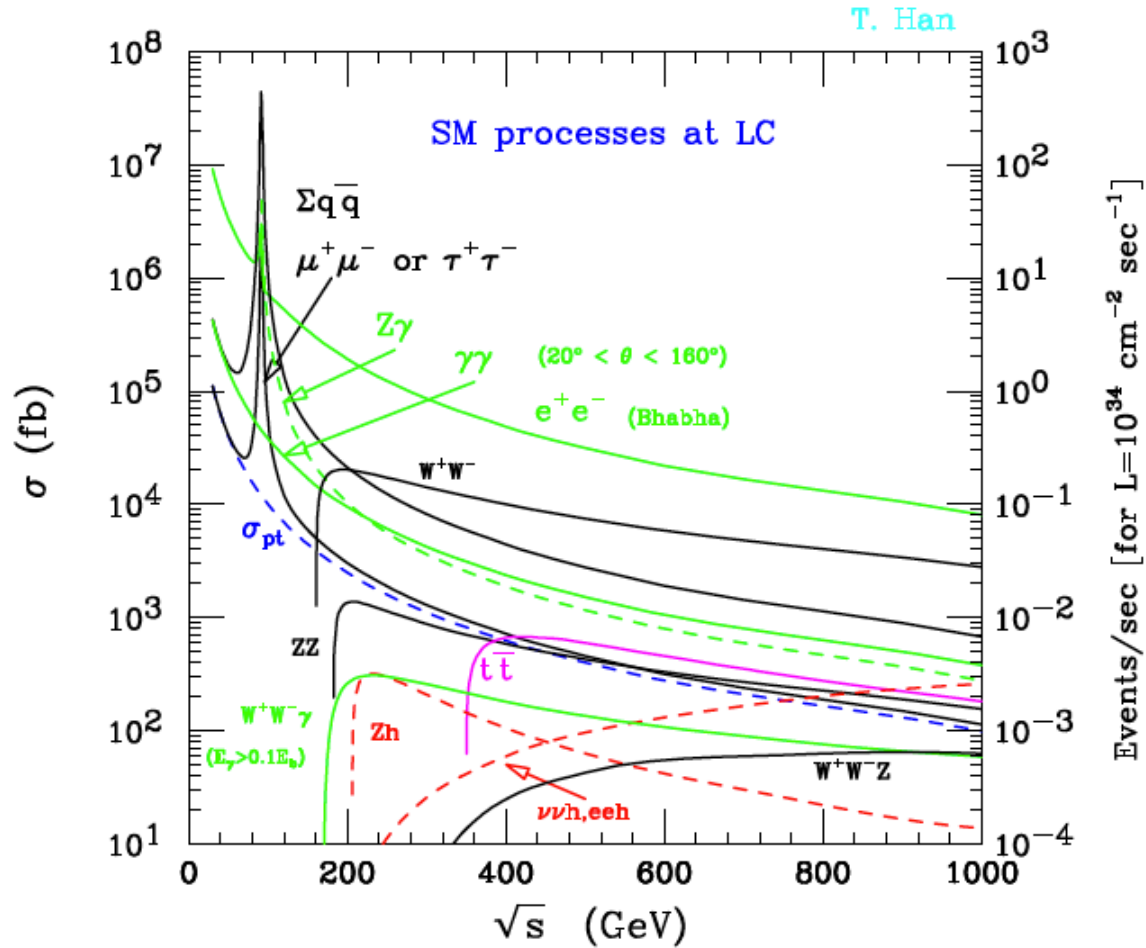
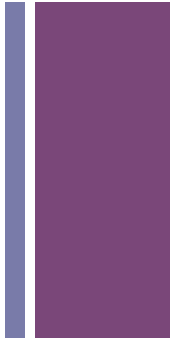
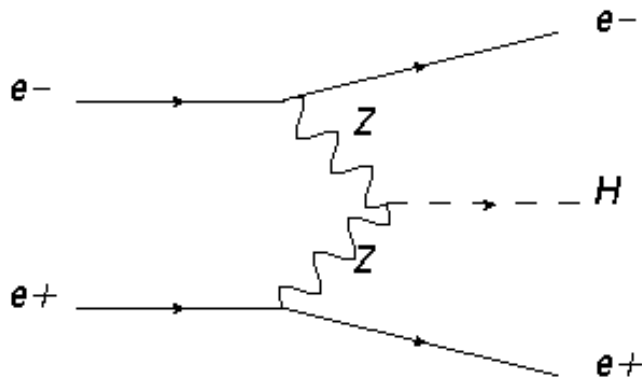
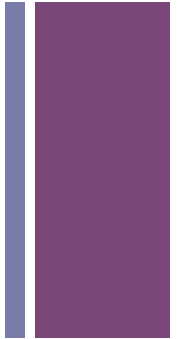


FIG. 2: Scattering cross sections versus c.m. energy for the SM processes in e^+e^- collisions. The Higgs boson mass has been taken as 120 GeV.



Signal and Background definition



Processes list:

- $e^- e^+ \rightarrow e^- e^+ h$
- $e^- e^+ \rightarrow e^- e^+ \nu \bar{\nu}$
- $e^- e^+ \rightarrow e^- e^+ q \bar{q}$
- $e^- e^+ \rightarrow e^- e^+ l^- l^+$
- $e^- e^+ \rightarrow e^- e^+ a a$
- $e^- e^+ \rightarrow e^- e^+ a$

Whizard 1.95 (ISR, Beam-strahlung) and Pythia (FSR, hadronization)
SGV – fast detector simulation

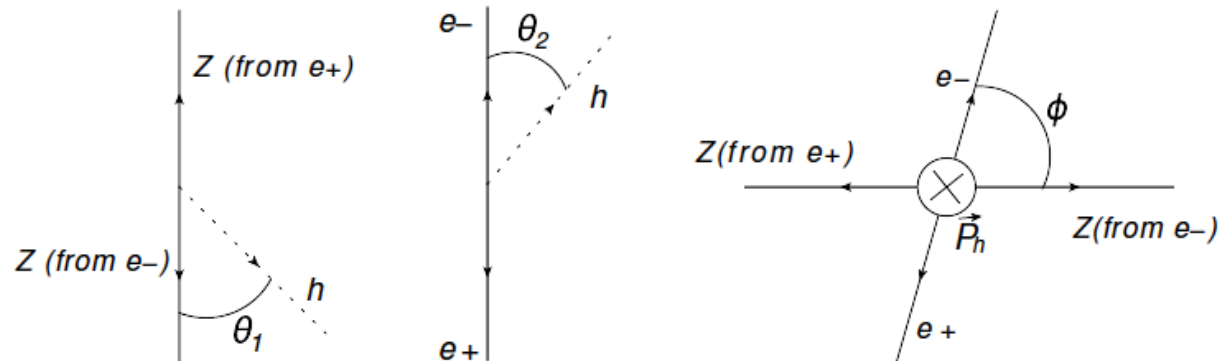


Kinematic Variables:

- m_{ee} : invariant mass of the outgoing $e^- e^+$ pair
- m_{rec} : recoil mass of the outgoing $e^- e^+$ pair

$$m_{rec}^2 \equiv s - 2\sqrt{s}E_{ee} + m_{ee}^2.$$

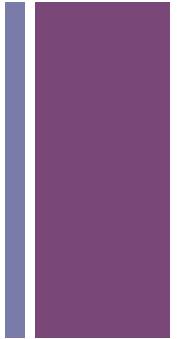
- θ_1 is the angle between the boosted momentum of the outgoing e^+e^- pair and the beam-line; θ_2 is the angle between the outgoing e^- in e^-e^+ rest frame and the momentum of e^+e^- pair in the lab frame; ϕ_3 is the azimuthal angle of the outgoing e^- relative to the plane defined by the outgoing e^+e^- pair and the beam-line in the lab frame.



+ Cuts and Distribution:

- Signal Identification:
 - recoil mass peak at Higgs mass;
 - Finite Pt of Higgs
- Dominant Backgrounds:
 - $e-e^+ \rightarrow W^-W^+ \rightarrow e\nu n l$
 - $e-e^+ \rightarrow eea$ (Bhabha scattering)

Cut 1	$95 \text{ GeV} < m_{\text{rec}} < 300 \text{ GeV}$ $500 \text{ GeV} < m_{ee} < 870 \text{ GeV}$ $p_{T(ee)} > 50 \text{ GeV}$ veto 1 iso. photon $E_{\gamma}^* < 200 \text{ GeV}$
Cut 2	$0.14 < \theta_2 < 3.0$ $\phi < 1.5$



■ Signal and background cross section (fb) at ILC 500 GeV

Process	Generator Level (fb)	Cut1 (fb)	Cut2 (fb)
$ee \rightarrow eeh(\text{Signal})$	11.5	3.48	3.11
$ee \rightarrow ee\nu_e\nu_e$	659	23.9	16.0
$ee \rightarrow ee\nu_{\mu,\tau}\nu_{\mu,\tau}$	78.6	1.02	0.70
$ee \rightarrow eeqq$	1850	9.33	6.88
$ee \rightarrow eell$	4420	5.18	4.42
$ee \rightarrow ee\gamma\gamma$	1640	1.18	0.60
$ee \rightarrow ee\gamma$	165000	1.32	0.66
Total Background	174000	41.9	29.2
$\delta\sigma/\sigma$	-	8.7%	8.2%

Sensitivity on the signal:
$$\frac{\delta\sigma}{\sigma} = \frac{\sqrt{N_s + N_b}}{N_s},$$

+ Distribution

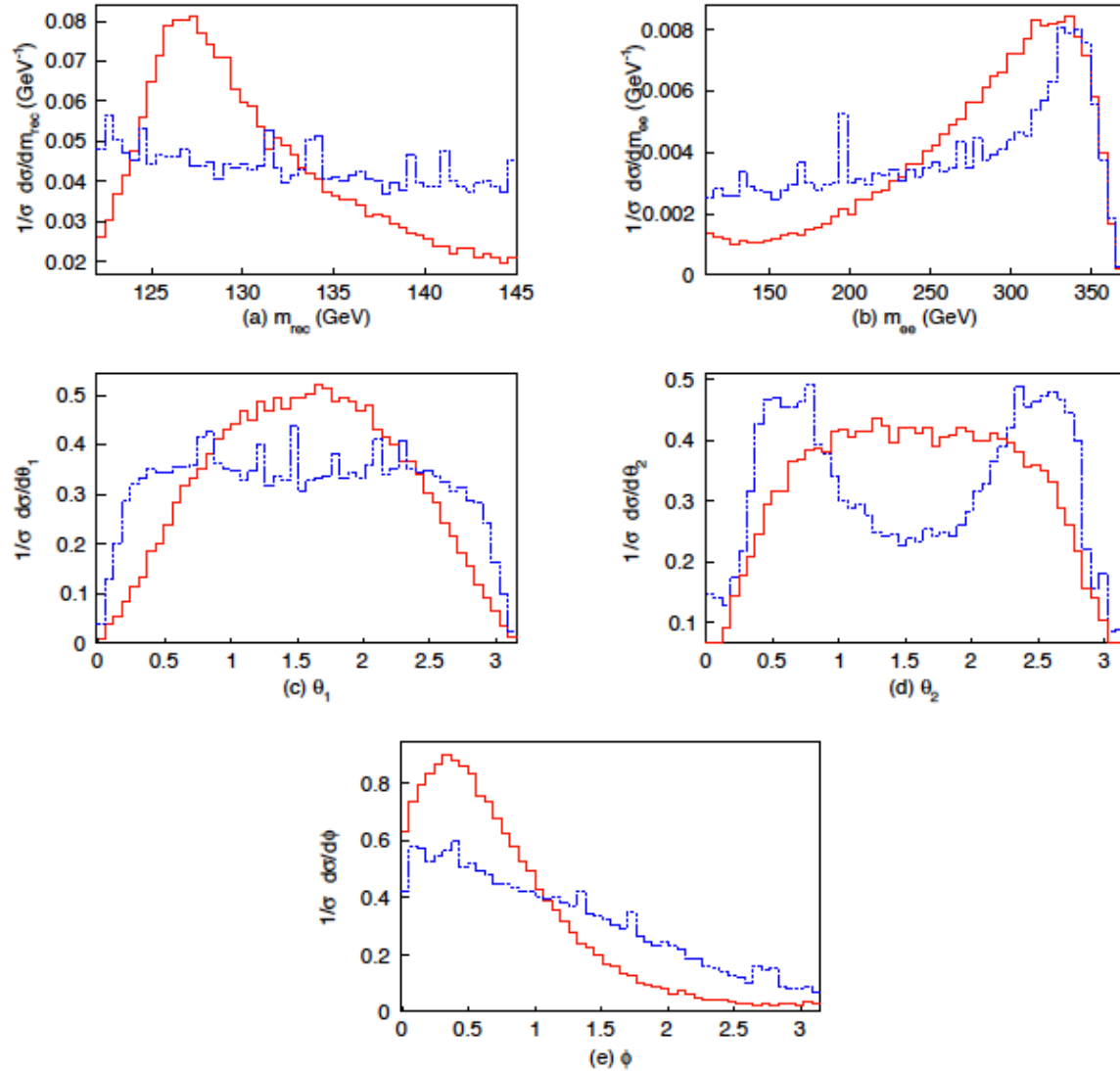


Figure 4. Comparison of signal (solid red) and total background (dashed blue) distributions for variables m_{rec} , m_{ee} , θ_1 , θ_2 and ϕ at $\sqrt{s} = 500$ GeV. Cut1 in Table 2 is applied. For clarity, both signal and background distributions are normalized to unity.



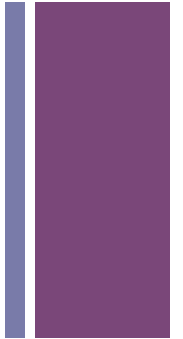
Similar analysis gives results for 1TeV case:

Cut 1	$95 \text{ GeV} < m_{\text{rec}} < 300 \text{ GeV}$ $500 \text{ GeV} < m_{ee} < 870 \text{ GeV}$ $p_{T(ee)} > 50 \text{ GeV}$ veto 1 iso. photon $E_{\gamma}^* < 200 \text{ GeV}$
Cut 2	$0.14 < \theta_2 < 3.0$ $\phi < 1.5$

Process	Generator Level (fb)	Cut1(fb)	Cut2(fb)
$ee \rightarrow eeh(\text{Signal})$	24.1	8.18	7.52
$ee \rightarrow ee\nu_e\nu_e$	978	31.5	17.2
$ee \rightarrow ee\nu_{\mu,\tau}\nu_{\mu,\tau}$	93.9	3.24	1.64
$ee \rightarrow eeqq$	2830	24.1	13.6
$ee \rightarrow eell$	6690	13.7	10.8
$ee \rightarrow ee\gamma\gamma$	3180	2.68	1.10
$ee \rightarrow ee\gamma$	175000	4.73	2.28
Total Background	189000	80.0	46.6
$\delta\sigma/\sigma$	-	3.6%	3.1%



Multivariate analysis: using log-likelihood



We can do slightly better by making use of the shape of distribution.

Define log-likelihood on the five-dimensional space:

$$LL_P(n_i; \nu_i) = 2 \sum_i \left[n_i \ln \left(\frac{n_i}{\nu_i} \right) + \nu_i - n_i \right]$$

Where in each bin:

- ν_i = expected value , background + signal
- n_i = background + r *signal
- The 1-sigma deviation corresponds to $LL = 1$.



Results of 1TeV log-likelihood

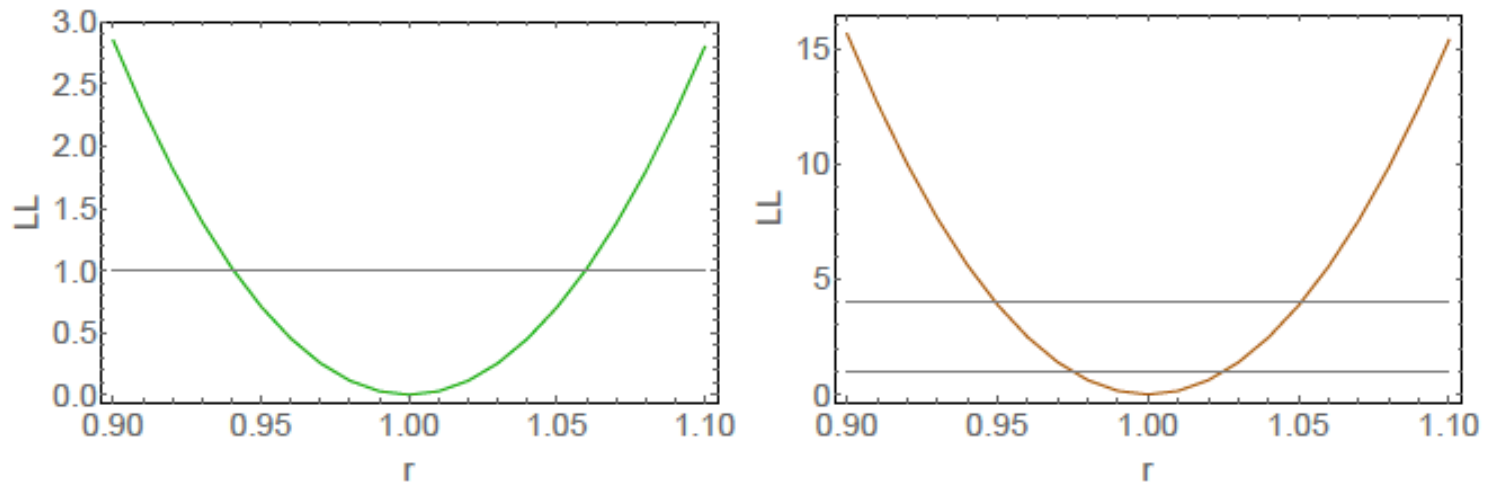
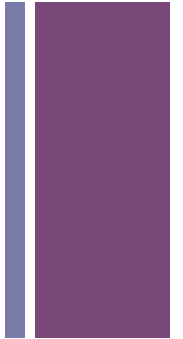
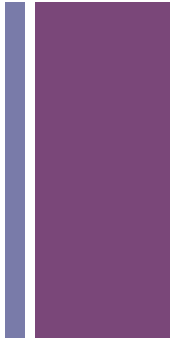


Figure 6. 5-dimensional Log-likelihood as a function of the relative cross section r defined below Eq. (2.5) for (left panel): 500 GeV case and (right panel): 1 TeV case. For both analyses, Cut1 is applied.

Sensitivity improved to 6%(2.5%) for the 500GeV(1TeV) using log-likelihood calculation.



Main Results: Improved sensitivity on Higgs width and couplings:



Relative Error %	ILC 250+500		ILC 250+500+1000	
$\delta\sigma_{Zh}$	6.0%		2.5%	
Improvement		with HL-LHC		with HL-LHC
Γ	4.8 \rightarrow 4.7	4.8 \rightarrow 4.6	4.5 \rightarrow 3.7	4.5 \rightarrow 3.7
g_Z	0.99 \rightarrow 0.94	0.99 \rightarrow 0.94	0.98 \rightarrow 0.75	0.98 \rightarrow 0.75
g_W	1.1 \rightarrow 1.1	1.1 \rightarrow 1.1	1.1 \rightarrow 0.89	1.1 \rightarrow 0.88
g_b	1.5 \rightarrow 1.5	1.5 \rightarrow 1.5	1.3 \rightarrow 1.2	1.3 \rightarrow 1.1

Table 6. The improvement on selected coupling precisions by incorporating our ZZ fusion analysis from a typical 10-parameter model-independent fit. We show both the ILC exclusive results and ILC combined with the optimistic CMS HL-LHC input [27]. For details of fitting scheme and combination scheme, see Ref. [16]. The results for ILC 250/500/1000 (GeV) assume 250/500/1000 fb^{-1} integrated luminosities.

+ Constraints on dim-6 operator:

From studying the ZZ fusion channel, we have now much more improved sensitivity to ZZh coupling at 500GeV and 1TeV c.m. energy:

We did some constraints on two representative dim-6 operators:

$$\mathcal{O}_H = \partial^\mu(\phi^\dagger\phi)\partial_\mu(\phi^\dagger\phi), \quad \mathcal{O}_{HB} = g' D^\mu\phi^\dagger D^\nu\phi B_{\mu\nu},$$

$$\mathcal{L}^{\text{dim-6}} \supset \frac{c_H}{2\Lambda^2}\mathcal{O}_H + \frac{c_{HB}}{\Lambda^2}\mathcal{O}_{HB},$$

$$\bar{c}_H = \frac{v^2}{\Lambda^2}c_H \quad \text{and} \quad \bar{c}_{HB} = \frac{m_W^2}{\Lambda^2}c_{HB}.$$

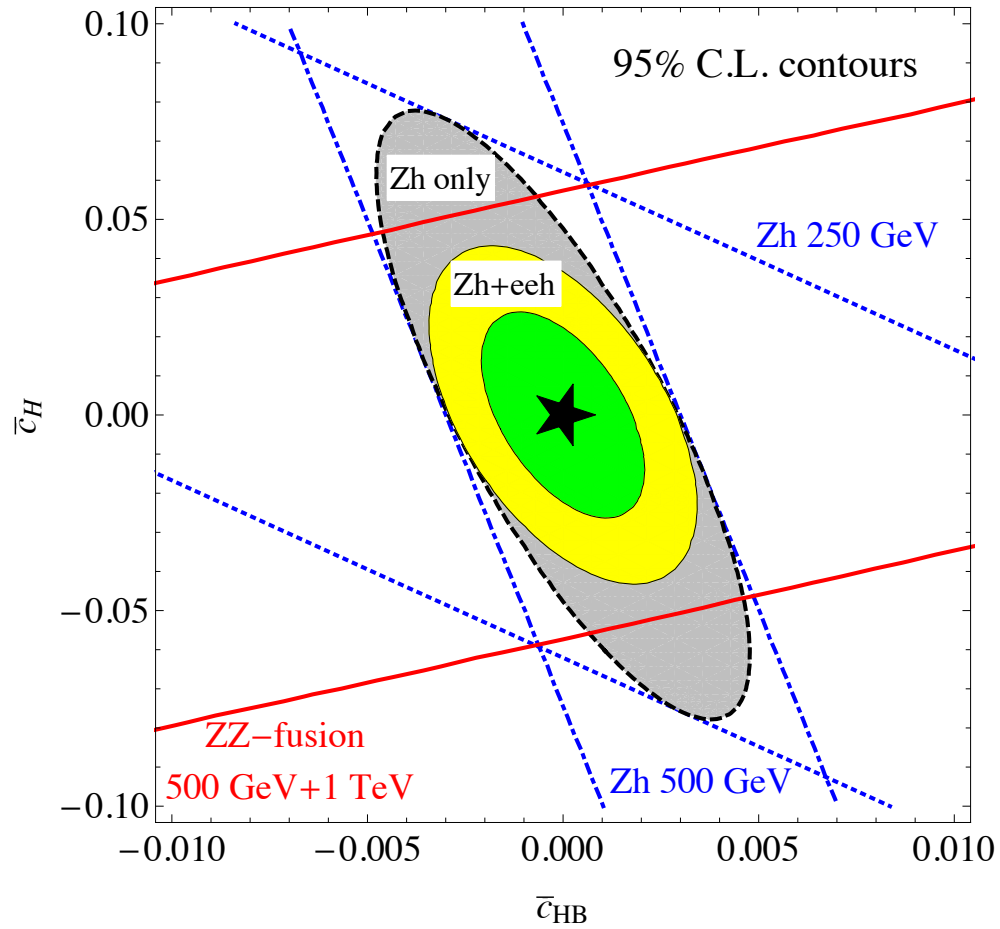
$$\text{ILC 250 GeV : } \frac{\Delta\sigma}{\sigma}(Zh) \approx -\bar{c}_H - 4.5 \bar{c}_{HB},$$

$$\text{ILC 500 GeV : } \frac{\Delta\sigma}{\sigma}(Zh) \approx -\bar{c}_H - 25 \bar{c}_{HB},$$

$$\frac{\Delta\sigma}{\sigma}(e^-e^+h) \approx -\bar{c}_H + 1.1 \bar{c}_{HB},$$

$$\text{ILC 1 TeV : } \frac{\Delta\sigma}{\sigma}(e^-e^+h) \approx -\bar{c}_H + 2.4 \bar{c}_{HB}.$$

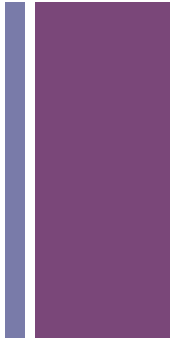
+ Constraints on dim-6 operator:

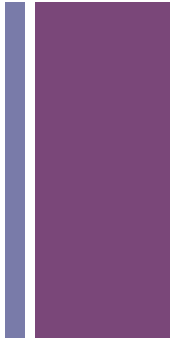




Final Remarks:

- Combing the ZZ fusion and Higgsstrahlung channels, the model-independent measurement of the inclusive cross section ZH can be improved to 1.5%, which is ~25% improvement over existing studies.
- Sensitivities on the inclusive cross section ZH at multiple energies at ILC offers the possibility to distinguish contributions from different BSM operators.
- As an example, we showed that by including the ZZ fusion channel, constraints on two representative operators improve as large as 50% compare to studies with Higgsstrahlung channel alone.





- Thank you for the attention.

+ Backup Plots: ZZ-fusion (1TeV)

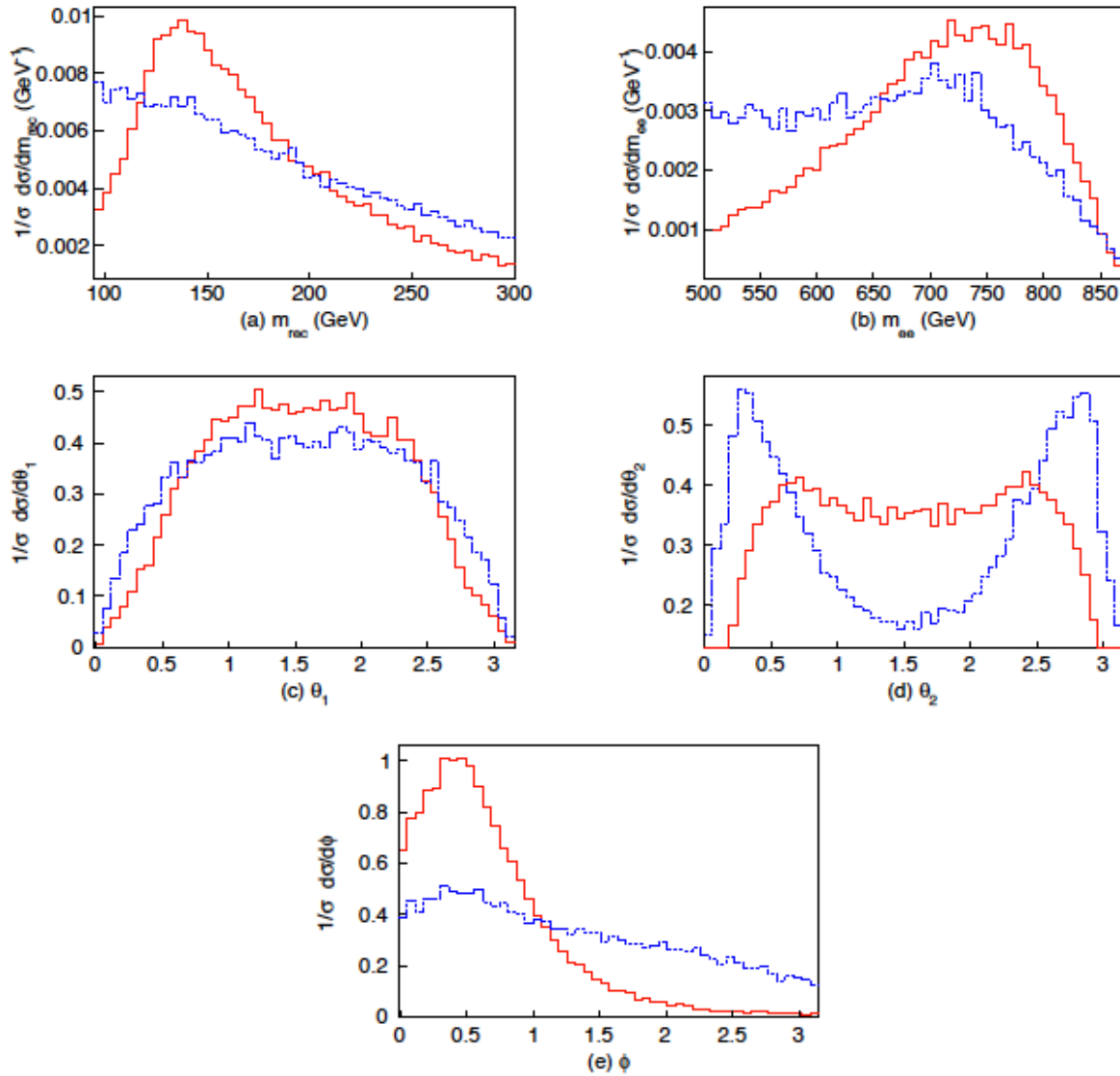


Figure 5. Comparison of signal (solid red) and total background (dashed blue) distributions for variables m_{rec} , m_{ee} , θ_1 , θ_2 and ϕ at $\sqrt{s} = 1$ TeV. Cut1 in Table 4 is applied. For clarity, both signal and background distributions are normalized to unity.

+ Backup: previous Studies on Higgs coupling constraints at ILC

Facility		ILC	
\sqrt{s} (GeV)	250	500	1000
$\int \mathcal{L} dt$ (fb $^{-1}$)	250	+500	+1000
$P(e^-, e^+)$	(-0.8, +0.3)	(-0.8, +0.3)	(-0.8, +0.2)
Γ_H	12%	5.0%	4.6%
κ_γ	18%	8.4%	4.0%
κ_g	6.4%	2.3%	1.6%
κ_W	4.9%	1.2%	1.2%
κ_Z	1.3%	1.0%	1.0%
κ_μ	91%	91%	16%
κ_τ	5.8%	2.4%	1.8%
κ_c	6.8%	2.8%	1.8%
κ_b	5.3%	1.7%	1.3%
κ_t	—	14%	3.2%
BR_{inv}	0.9%	< 0.9%	< 0.9%

$$\kappa_Z = \frac{g_{ZZH}}{g_{ZZH}^{SM}}$$

+ Backup: BSM model on Higgs coupling

Table 1-8. *Generic size of Higgs coupling modifications from the Standard Model values when all new particles are $M \sim 1$ TeV and mixing angles satisfy precision electroweak fits. The Decoupling MSSM numbers assume $\tan \beta = 3.2$ and a stop mass of 1 TeV with $X_t = 0$ for the κ_γ prediction.*

Model	κ_V	κ_b	κ_γ
Singlet Mixing	$\sim 6\%$	$\sim 6\%$	$\sim 6\%$
2HDM	$\sim 1\%$	$\sim 10\%$	$\sim 1\%$
Decoupling MSSM	$\sim -0.0013\%$	$\sim 1.6\%$	$\sim -0.4\%$
Composite	$\sim -3\%$	$\sim -(3 - 9)\%$	$\sim -9\%$
Top Partner	$\sim -2\%$	$\sim -2\%$	$\sim +1\%$